Journal of Nepal Geological Society, 2023, Vol. 66, pp. 75–90
https://doi.org/10.3126/jngs.v66i01.57933

Numerical modelling of cut-slope stability in the Lesser Himalayan terrain of West-central Nepal

Krishna Kumar Shrestha[1], Kabi Raj Paudyal[1], and Prem Bahadur Thapa[2,*]

[1]Central Department of Geology, Tribhuvan University, Kirtipur, Kathmandu, Nepal
[2]Department of Geology, Tri-Chandra Multiple Campus, Tribhuvan University, Kathmandu, Nepal
**Corresponding author's email: prem.thapa@trc.tu.edu.np*

ABSTRACT

Area development without due consideration of geological factors has led to recurrent slope failures within the Lesser Himalayan Zone thereby rendering socio-economic impacts. This issue is well exemplified by cut-slopes in major highways of Nepal traversing through a diverse range of rocks and soils. The study has focused on addressing the stability challenges posed by highly vulnerable excavated cut-slopes with particular attention given to a debris cut-slope considered as a model for this study, located in the Lesser Himalayan terrain of west-central Nepal. The cut-slope model is analyzed by numerical modellings through both the limit equilibrium method (LEM) and finite element method (FEM). The study further evaluated the underlying causes of these failures to recommend the options for remedial measures. Data acquired from two-dimensional electrical resistivity tomography (2D-ERT), multi-channel analysis of surface waves (MASW) and laboratory testing were integrated into numerical modelling and simulation. The results showed that the lower slope below the natural benching is stable whereas the upper failed slope is unstable due to reduced gravitational loading. In LEM, factors of safety (FoS) range from 0.77 to 0.89 for cut-slope angles of 70° and 60° whereas the FoS in modified slopes (50° and 40°) were slightly greater than 1 which ranged from 1.01 to 1.18 and indicated marginal stability. Application of 25 mm diameter soil nails, each measuring 6 m in length and spaced at 2 m intervals with tensile and plate capacity of 125.6 kN, bond strength of 75.4 kN/m, and 80% of nail length have produced FoS of 1.30 or greater in LEM and FEM which is acceptable values specified by EM 1110-2-1902 and IS 456 2000 for end-of-construction and multistage loadings.

Keywords: Cut-slopes, Lesser Himalaya, slope stability, factor of safety, numerical modelling

Received: 12 March 2023 **Accepted:** 17 June 2023

INTRODUCTION

In mountainous regions such as the Himalayas, roads are commonly built by cutting and modifying natural slopes. The construction of roads and widening projects has notably degraded the stability of road cut-slopes (Siddique et al., 2017; Siddique et al., 2015; Pradhan et al., 2020; Siddique, 2018). The unregulated excavation of rocky slopes during road development and expansion exposes these slopes to heightened vulnerability (Singh et al., 2013; Sutejo and Gofar, 2015). Additionally, the presence of steeper cut-slopes along roads increases the likelihood of failure in the exposed rock formations (Umrao et al., 2011). Many instances of slope failures in engineered landscapes result from the gradual weakening of soils and soft rocks (Kharel and Acharya, 2017), augmented by rainfall (Dahal et al., 2006; Dahal, 2012). These materials may initially appear stable shortly after construction or excavation but eventually become prone to instability over time (Miščević and Vlastelica, 2014). In some cases, particularly for cut-slopes, failures can be attributed to design miscalculations, such as improper slope angles, excessive slope heights, and underestimated soil strength (Valentino et al., 2021; Singh et al., 2020).

There exist varieties of numerical methods to analyze the stability of natural and cut-slopes that include the slice method, rigid body limit equilibrium method, plastic limit analysis method, etc. (Li and Wang, 2007). Limit equilibrium methods (LEM) first define a proposed slip surface (SS) then the slip surface is examined to obtain the factor of safety, which is the ratio between the resisting moments and the driving moments along the slip surface. The finite element method (FEM) is a robust computational technique widely applied in engineering for simulating real-world phenomena. It excels by enabling the accurate simulation of complex physical behaviours without necessitating excessive simplifications. Particularly, complex engineering issues demand the finite element method to achieve dependable and precise outcomes. Contemporary engineering analysis techniques are often validated by the results obtained through the finite element method as a benchmark (Duncan, 1996; Stark et al., 2005).

Among many methods for slope stability analysis, the gravity increase method (Swan and Seo, 1999) and strength reduction method (Matsui and San, 1992) are considered the most widely used methods. The gravity increase method is used to study the stability of embankments during construction since it gives more reliable results while the strength reduction method is applied to study the stability of existing slopes (Albataineh, 2006). Wei et al. (2020) adopted a non-linear Stress Reduction Method (SRM) utilizing the generalized Hoek-Brown (GHB)

criterion to assess the potential failure of rock slopes. A discrete element modeling approach known as DSDM was utilized to analyze jointed rock slopes, incorporating SRM principles (Wang et al., 2019). Meanwhile, Yang et al. (2019) also developed a 3D-NSRNMN method, which uses a non-linear GHB failure criterion to evaluate the stability of rock slopes. The constant boundary element method discretizes the sliding mass to study the slope instability criteria related to SRM (Nie et al., 2019). Dynamic stability evaluation method integrates the dynamic considerations and an overall strength reduction method for stability assessments and support analyses for slopes (Chen et al., 2014). This strength reduction method has exactly the same definition as of the limit equilibrium methods (Griffiths and Lane, 1999) and has now become the mainstream method to analyze the displacement, stress and stability of slopes.

Slope stability analysis is based on the principle of FEM strength reduction method on both natural and excavated conditions with the application of support system to solve the practical construction problems in an optimized design system (Chhen et al., 2022; Pradhan et al., 2014). The safety factor is found to be incremented by 24.3% after the application of anchor rod and anchor cable reinforcement (Chhen et al., 2022) A numerical simulation of slope by strength reduction method is used to know the influence of piles and steel nails on slope stability (Fawaz et al., 2014). Rows of piles and steel nails applied for the modelled cut-slope have indicated the improvement in the factor of safety significantly. Nowadays, soil nailing is widely used as a reinforcement technique to improve the stability of steep slopes and vertical cuts (Fan and Luo, 2008; Jaiswal et al., 2022; Lin et al., 2013; Pandey et al., 2021; Zhang et al., 2014). The increase of L/H (ratio of soil nail to height of the slope) from 0.5–0.9 increases the factor of safety by 16.2–33.8% for slopes varying within 45°–90°, whereas the increase of L/H from 0.9–1.2 increases the factor of safety by only 1.7–4.3% (Elahi et al., 2022).

To address the stability of cut-slopes with respect to slope geometry, intrinsic properties and groundwater conditions, the present study has focused on the numerical modelling of cut-slopes along the Prithvi Highway of Nepal where road widening has created freshly excavated cut-slopes within differential soil compositions. The numerical results of the limit equilibrium and finite element methods were verified with the actual failed slope in order to know the cause of failure and to recommend possible remedial measures.

SETTING OF THE AREA

The modelling site of present study is located at Yampa village (27°56'42.72"N, 84°26'43.24"E) of Tanahun District in west-central Nepal (Fig. 1). The cut-slope is exposed along the Prithvi Highway and is 123 km west of Kathmandu, the capital city of Nepal. A road expansion project is currently in progress along the highway which has created numerous fresh cut-slopes. More than 60% of the cut-slopes along the Highway lie within debris materials and are vulnerable to failures. A major concern has been given to the foremost unstable cut-slopes which have a direct impact on road cut-slope stability.

Geologically, the cut-slope is found to be within the Dadagaon Phyllite of the Lesser Himalayan Zone (Fig. 2). Debris materials are exposed in the vicinity of area and geo-materials of the cut-slope comprise the multi-layers of soil with variations of properties. The materials consist of silty sand at the top, gravelly sand at the middle, and silty sand with gravel at the bottom (Fig. 3). The top layer is the residual soil whereas the middle and bottom layers are colluvium which is the transported debris from nearby hills and reworked by fluvial

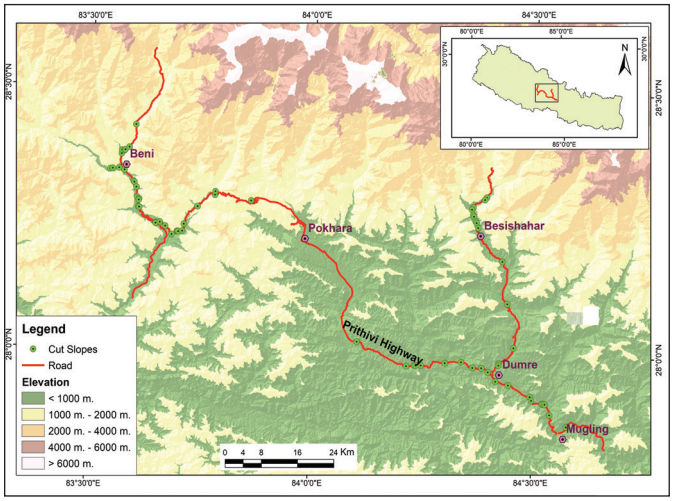

Fig. 1: Spatial distribution of cut-slopes along the Prithvi Highway and its feeder roads, west-central Nepal.

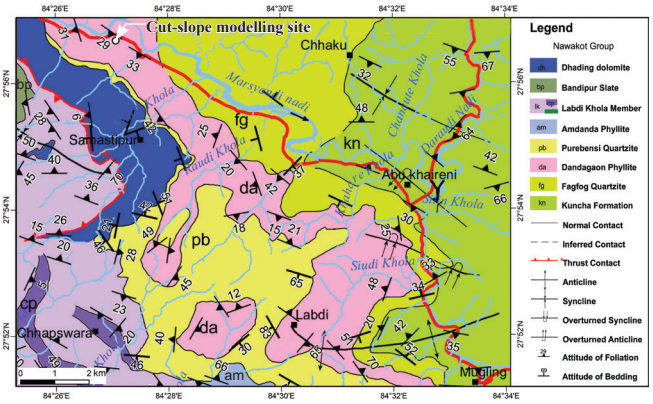

Fig. 2: Geological map of Mugling-Anbu Khaireni area showing cut-slope modelling site (modified after Paudyal and Paudel, 2011).

Fig. 3: Cut-slope excavated on debris material along the roadside at Yampa village, Prithvi Highway.

action. The average height of this cut-slope is 42 m from the existing road level and the slope is facing due north with a slope angle of 64°.

MATERIALS AND METHODS

The methodology consists of geotechnical investigation supported by geological and geophysical investigations to identify the soil properties. Sub-surface data for slope stability analysis were acquired by geophysical surveys including 2D-electrical resistivity tomography (ERT) (Loke and Lane, 2004) and multi-channel analysis of surface waves (MASW) (Park et al., 1999) were conducted at the top of the existing cut-slope to verify the different soil layers and also to determine the dynamic properties of the soils. Furthermore, laboratory experiments were carried out to determine the strength parameters of slope materials. The data from field investigations and laboratory tests were used to evaluate slope stability conditions based on the limit equilibrium method and finite element methods.

Geotechnical and geophysical field survey

An inventory map of excavated cut-slopes along the Prithvi Highway from Beni to Mugling was prepared (Fig. 1). This involved extracting the existing geometric features of the cut-slopes along with their inherent characteristics. The consistent presence of groundwater for a certain layer of modelling site of cut-slope throughout the year prompted investigative efforts to assess their stability. Subsequently, comprehensive geotechnical and geophysical investigation surveys were conducted to provide a detailed database of soil properties. Samples (S1, S2, S3) were collected from three different layers to assess their geotechnical characteristics in relation to slope stability.

To determine and verify the thickness of various soil layers along the cut-slope and to identify the groundwater level (GWL), a two-dimensional electrical resistivity tomography (2D-ERT) survey of 300 m long profile was performed. Additionally, three multi-channel analyses of surface waves (MASW) survey were carried out at an average span of 80 m on the top flat surface of the cut-slope to determine soil layers and their dynamic properties. For 2D-ERT, the data acquisition was made using state-of-the-art technology equipment, WDJD-4 Resistivity & IP Sounding Meter. This ERT profile was extended for 300 m with 60 electrodes at 5 m intervals applying Wenner-α array to obtain the subsurface information up to 60 m deep from the top surface of the cut-slope. Similarly, a 24-channel ABEM Terraloc Pro 2 seismograph was used, fitted with vertical geophones of 4.5 Hz frequency to capture the shear wave velocity (Vs) produced by an active source, specifically a 10 kg hammer striking a rubber plate. The dynamic modulus of soil or rock characteristics was computed based on the acquired Vs.

The dynamic modulus of soils represents how the material responds to dynamic loading, such as vibrations or seismic waves (Shah et al., 2023; Towhata, 1996; Lentil et al., 2008; Zainorabidin et al., 2015). It reflects the soil's ability to transmit stress and deformations under these conditions. In soils, the shear wave velocity is influenced by factors like the soil's stiffness, density, and confining pressure. Both geophysical methods, 2D-ERT and MASW show that there are four horizontal layers of varying compositions along the modelling cut-slope at Yampa village (Fig. 4, 5). The utilization of this information has played a significant role in the process of validating the depth and thickness of compositional layers present in the cut-slope model, thereby facilitating the formulation of numerical simulations.

The shear modulus outlines how a material reacts to shear stress. Many seismic geophysical tests produce slight shear strains, and the recorded shear wave velocity (Vs) can be leveraged to calculate the highest attainable dynamic shear modulus or soil stiffness (G_{max} or G_o) with a knowledge of the soil's density (ρ) (Strelec et al., 2016) as shown in Equation 1.

$$G_o = \rho * V_s^2 \quad (1)$$

The soil density ρ can be evaluated from the measured shear-wave velocity V_S and the depth h (Eq. 2).

$$\rho = 0.85 \cdot \log(V_s) - 0.16 \log(h) \quad (2)$$

A small strain shear modulus is the key benchmark and establishes the highest, achievable soil stiffness that other moduli can be compared to on a relative basis.

The Young's modulus E_o describes the material's response to linear stress. Its relation to the shear modulus G_o is defined in Equation 3.

$$E_o = 2 * G_o(1+\upsilon) \quad (3)$$

where, υ is the Poisson's ratio which can be expressed in terms of properties that can be measured in the field (Eq. 4), including velocities of P-waves (V_p) and S-waves (V_s).

$$\upsilon = \tfrac{1}{2} (V_p^2 - 2V_s^2) / (V_p^2 - V_s^2) \quad (4)$$

Porosity (n) can be defined in terms of P-wave velocity (Kassab and Weller, 2014) as per the relationship (Eq. 5).

$$n = 0.175 \ln (V_p) + 1.46 \quad (5)$$

According to Weingarten and Perkins (1995), empirical relationship between internal friction angle (ϕ) in terms of porosity (n) for compact soil and soft bedrock can be expressed as in Equation 6.

$$\phi = 57.8 - 105(n) \quad (6)$$

Soil characterization

The distribution of grain sizes in debris materials holds insights into their engineering characteristics to a certain extent. It

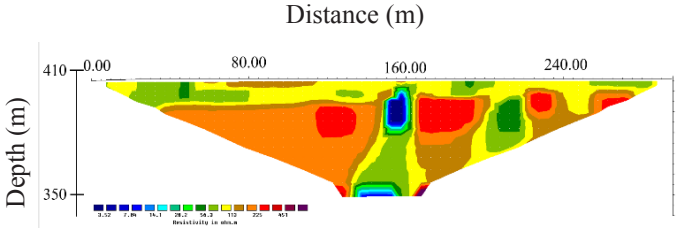

Fig. 4: Interpretative 2D-ERT image showing differentiation of soil layering.

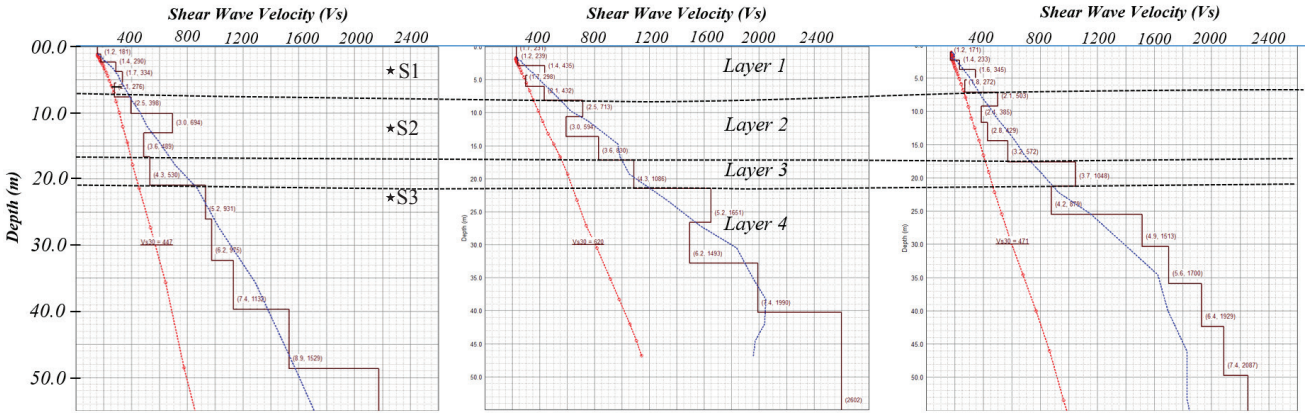

Fig. 5: Shear wave velocity versus depth profile for MASWs along top of the modelling cut-slope. ⋆ *Denotes location of sampling.*

assists in categorizing soil types based on their impact on the stress-strain dynamics and strength of the materials that constitute a slope. To determine this distribution, the dry sieving method was adopted in accordance with established practices. The outcomes of this analysis were utilized to classify the fine-grained fraction following the Unified Soil Classification System (USCS). Additionally, a density test, conforming to standard protocols, was conducted. By performing three sets of tests on collected soil samples, the unit weight of the soil was calculated.

The Poisson's ratio of the soil materials was taken from relevant literature about the debris materials in the Himalayan region. This was done considering the elasto-plastic nature of the materials, which aligns with Mohr-Coulomb failure criterion. It was then juxtaposed with the Poisson's ratio derived from shear wave velocity (Vs) data obtained through the multichannel analysis of surface waves (MASW) survey.

Furthermore, various samples tested by direct shear tests to evaluate key shear strength parameters–specifically, cohesion (c) and the angle of internal friction (ϕ) (Table 1). These evaluations adhered to the procedures outlined in IS: 2720 (Part 13). Given that failure predominantly occurs during the monsoon season in the study area, the tests were conducted under drained saturated conditions, which shows the most unfavorable soil scenario. Three direct shear tests were conducted on slope materials, applying three distinct normal stresses–0.5 kg/cm², 1.0 kg/cm², and 1.5 kg/cm²–while keeping a shearing rate of 0.01.

These specific normal stresses were considered to compute the soil's effective stress and failure threshold under the most challenging soil conditions (characterized by the lowest safety factor achieved under normal stress). The shear stresses at the point of failure were then plotted against each corresponding normal stress value of 37.6 kPa, 72.4 kPa, and 89.8 kPa. Utilizing the resulting graph, the cohesion and angle of internal friction for the materials were calculated, in accordance to the Coulomb failure criterion as expressed in Equation 7.

$$\tau = \sigma \tan(\phi) + c \quad (7)$$

where, τ represents the ultimate shear stress at the point of failure, σ denotes the normal stress at the failure plane, ϕ indicates the angle of internal friction, and c signifies the apparent cohesion of the soil sample.

Table 1: Engineering properties of the samples from successive soil layers of cut-slopes (see Fig. 5).

ID	DST		BD, gm/cc (compacted)		GSA (%)		
	ϕ	c (kPa)	Dry	SSD	Fine	Sand	Gravel
S1	33°	13.72	1.350	1.405	17.51	82.50	0.00
S2	32°	7.84	1.739	1.795	5.89	40.80	53.40
S3	33°	18.63	1.457	1.507	13.96	58.40	27.60

DST = Direct Shear Test, BD = Bulk Density, SSD = Saturated Surface Dry, GSA = Grain Size Analysis

Cut-slope stability assessment

For the slope stability assessment in this study, the Rocscience Slide v6.005 software's limit equilibrium method was applied. LEMs are techniques used for analyzing slope stability, and they can be categorized into rigorous and non-rigorous methods. The rigorous methods, namely those developed by Spencer (Spencer, 1967) and Morgenstern and Price (Morgenstern and Price, 1965), were chosen for their accuracy as they consider any shape of slip surface and fulfill complete equilibrium conditions. The non-rigorous methods include Ordinary/Fellenius (Fellenius, 1936), Bishop simplified (Bishop, 1955) and Janbu Simplified (Janbu, 1954) as these methods are applicable only to circular failures surfaces and only consider the overall moment equilibrium.

The input parameters required for the analysis were obtained from laboratory test results and geophysical survey result. The Mohr-Coulomb parameters were calculated using direct shear strength tests conducted on disturbed soil samples, with pebble-sized particles manually removed to meet the shear box requirements (6 cm × 6 cm). This removal process might introduce minor discrepancies in the representative shear strength parameters may lead to some uncertainties in the results.

In this study, the shear strength parameters (cohesion and friction angle) of the overburden, along with the unit weight were treated as random variables in the analysis. Furthermore, the literature review of analogous samples was used to take into account the permeability of various soil layers.

In order to compare results of limit equilibrium methods with finite element analysis results, strength reduction method was selected in this study since it resembles the limit equilibrium

approach more than the gravity increase method. In finite element slope stability analysis, the use of the strength reduction method with advanced soil models leads to a behavior similar to the Mohr–Coulomb model since stress-dependent stiffness behavior and hardening effects are excluded (Sharma et al., 2017; Singh et al., 2013; Pradhan and Siddique, 2018). In advanced constitutive soil models, stiffness modulus is stress-dependent and changes based on step-size computation increments. When strength reduction method is used stiffness modulus from the previous step is used as a constant stiffness modulus during computations, and as a result, the advanced soil model behaves like the Mohr–Coulomb model where a constant stiffness modulus is used as well (Brinkgreve et al., 2013).

The Mohr–Coulomb model needs six parameters as input; friction angle (ϕ), cohesion (c), dilation angle (Ψ), deformation modulus (E), Poisson's ratio (ν), and unit weight (γ). For slope stability analysis, $\Psi = 0$ was adopted assuming a non-associated flow rule, based on the results by Griffiths and Lane (1999). Young's modulus and Poisson's ratio are of insignificant importance in slope stability analysis using strength reduction method, due to the nature and mathematical formulation of the method (Matsui and San, 1992).

As part of the analysis focused on trial slip surfaces, a range of limit equilibrium models were assessed to determine their respective minimum factors of safety (FoS). These models were constructed based on site measurements and incorporated material properties to compute the deterministic FoS for each LEM. This comprehensive process involved a meticulous consideration of various factors, including material characteristics and the potential risks linked to each LEM. Through a detailed examination of each LEM, any inherent weaknesses or susceptibilities that could result in failure or other complications were identified. Ultimately, this analysis played a pivotal role in ensuring that the final product would be secure, dependable, and efficient, while minimizing the potential risk of failures.

Ordinary Fellenius method

In situations where the angle of shearing resistance remains inconsistent along the failure surface, such as in zoned earth dams where the failure plane can cross different materials, the conventional friction circle approach is not suitable. In these cases, a more appropriate method is the 'slices' approach. This technique involves vertically dividing the sliding wedge. To calculate the factor of safety, it is necessary to examine the individual contributions of each slice in terms of the forces that promote sliding and those that resist it.

These forces include the slice's own weight (W), the forces applied to the lower boundary in both vertical and horizontal directions, and the lateral forces denoted as X and E, which act on the slice's sides. In the Ordinary method of Slices, also known as the Fellenius method or the Swedish Circle method (Fellenius, 1936; May and Brahtz, 1936), several simplifications are incorporated to render the problem manageable and solvable.

Initially, it's assumed that we can ignore the lateral forces X and E. Secondly, it's suggested that we can find the normal force N by breaking down the weight of the slice W into a direction perpendicular to the arc, right at the middle of the slice. The factor of safety is calculated by Equation 8 (Fellenius, 1936).

$$F = \frac{\Sigma(c'\Delta X \sec\alpha + \tan\phi'(W\cos\alpha - u\,\Delta X \sec\alpha))}{\Sigma W \sin\alpha} \quad (8)$$

where, α is the angle of inclination of the potential failure arc to the horizontal at the mid-point of the slice.

Bishop Simplified

The simplified Bishop Method (Bishop, 1955), derived from the slice based approach in limit equilibrium analysis (Fig. 6a), has been implemented using Slide v.6 software. This method primarily considers both pore water pressure and the impacts exerted on the sides of individual slices (Fig. 6b).

In this approach, it is assumed that there is no pore water pressure, and the normal and tangential forces acting on the slice are considered to be equal in magnitude to the resultant forces of nearby slices.

At equilibrium condition, the factor of safety (FoS) for a slope is computed using Equation 9 (Bishop, 1955).

$$F_s = \frac{\sum_{n=1}^{n=p}[C\Delta L_n \cos\alpha_n + ((W_n - U\cos\alpha_n) + \Delta T)\tan\phi]\frac{1}{m_a}}{\sum_{n=1}^{n=p} W_n \sin\alpha_n} \quad (9)$$

where,

$$m_a = \cos\alpha_n + \frac{\tan\phi \sin\alpha_n}{F_s}$$

c = cohesion, ϕ = internal friction angle, W_n = weight of the n^{th} slice, ΔL = increase in width of the n^{th} slice, U = the boundary water force.

The factor of safety (FoS) is a measure of the safety level attained across the trial slip surface. This method is particularly suitable for circular failure patterns (Bishop, 1955). It is very useful for assessing the stability of slopes composed of unconsolidated geomaterials such as soil or debris. Thus, this approach of LEM can also yield valuable result in evaluating the FoS for the modeled cut-slope of this present study.

Janbu simplified and corrected

Janbu's simplified method can be employed for non-circular slip surfaces. This method assumes that the forces between slices are horizontal, resulting shear forces being considered as zero.

The factor of safety equation in this case is: $F = f_0.F_0$

where, F_0 is the factor of safety in a simplified case and a correction factor f_0 introduced to consider the effects of interslice shear forces (Janbu, 1954) (Eq. 10).

$$f_0 = 1 + b_1\left[\frac{d}{L} - 1.4\left(\frac{d}{L}\right)^2\right] \quad (10)$$

where, d is the maximum vertical distance between line segment and failure surface, L=length of slip surface.

For c-only soil, b_1=0.69, for c and ϕ soil, b_1=0.5, for ϕ only soil, b_1=0.31.

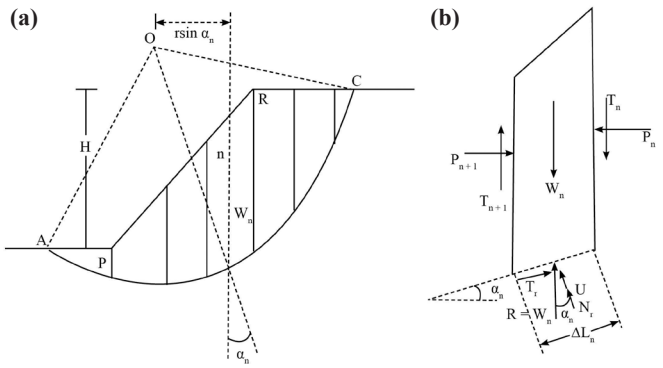

Fig. 6: Simplified Bishop's method (Bishop, 1955) (a) slices of soil above failure plane, (b) forces acting on side of a typical slice.

Based on the cohesion (c) and friction angle (ϕ), correction factor has been introduced to calculate the factor of safety. In Janbu correction, factor of safety is calculated (Bishop, 1955) (Eq. 11).

$$F = fo \frac{\sum_{i=1}^{N} C_i \times B_i + \sum_{i=1}^{N} W_i \cos(\alpha_i).\tan(\phi_i) - \sum_{i=1}^{N} U_i \cos(\alpha_i).\tan(\phi_i)}{\sum_{i=1}^{N} W_i \cos(\theta_i).\sin(\theta_i)} \quad (11)$$

where, α_i= angle of inclination made by failure surface to horizontal, c_i= cohesion, ϕ_i= internal friction angle, w_i= weight of the i-slice, U_i= boundary water force, B_i= width of i-slice, θ= inclination of resultant force.

Spencer method

Spencer's method was initially designed for the analysis of circular slip surfaces. However, it was subsequently adapted to handle non-circular slip surfaces by introducing the concept of a frictional center of rotation. This method operates under the assumption that the forces between adjacent slices are parallel to each other and have the same inclination. The factor of safety for the Spencer method is given in Equation 12 (Spencer, 1967).

$$F = \frac{\Sigma(c'l + (P - ul)\tan\phi')\sec\alpha}{\Sigma(W - (X_R - X_L))\tan\alpha} \quad (12)$$

where, c'=effective cohesion, l = length of each slice, W = weight of the slice, p = effective normal force acting on the base of the slice, u = pore water force.

Morgenstern-Price method

The Morgenstern-Price method is a rigorous approach for stability calculations that fully accounts for moment equilibrium (Fan et al., 2021). FoS for this method is calculated by Equation 13.

$$F = \tan\phi_i \tan(\delta_{i+1} - \alpha_i) \quad (13)$$

$$\delta_i = \lambda f(x_i)$$

where, ϕ_i= angle of internal friction of soil on the slip surface segment, α_i= inclination of the slip surface segment

RESULT AND DISCUSSION

Geotechnical characteristics of materials

The grain size distribution of a soil profile, which is predominantly composed of coarse fractions. The grain distribution curves shows that the soil has a meagre fine-grained fraction ranging from 5–18%, indicating unfavorable conditions for their formation or their entrainment by runoff into streams. The debris material was classified as well-graded sands, gravelly sands, with little fines suggesting that particle size distribution has little or no influence on the mechanical behavior of slope materials. The direct shear test results of all samples were expressed in terms of the linear Mohr-Coulomb failure criterion. Based on the regression equations, the calculated friction angle and cohesion of the debris range from 32° to 33° and 8–19 kPa respectively (Table 2). This suggests that the soil has critical stability and is prone to sliding under disturbed conditions.

Table 2: Input parameters for stability analysis.

S.N.	Material type	Unit weight γ (kN/m³)	Cohesion (c) kPa	Friction angle (ϕ)°	Permeability (KS), cm/s
1.	Silty Sand	16	14	33	0.0001
2.	Sandy Gravel	19	8	32	0.1
3.	Silty Sand with Gravel	19	19	33	1e-005
4.	Breast Wall	24			1e-007

Dynamic properties of the different layers as delineated by the shear wave velocity (Vs) were presented in Figure 7 to observe the soil properties before laboratory tests of samples. The reliability of the laboratory results can be cross-checked with the help of dynamic parameters calculated on the basis of shear wave velocity (Vs).

Slope stability analysis

Limit Equilibrium Method (LEM)

The modelled cut-slope at Yampa village of Prithvi Highway consists of two distinct sections: the upper portion, which has experienced a failure, and the lower part, which has remained stable. The instability of the upper section prompted modifications to be made. According to the limit equilibrium method (LEM), specifically the Fellenius method by adopting the geotechnical properties calculated from the shear wave velocity (Fig.7), the lower bench with its compacted mass exhibits a FoS of 1.15 (Fig. 8). This value indicates that the slope is marginally stable.

The slope stability assessment on modified failed slope (Fig. 9) based on limit equilibrium methods (LEMs) (Singh et al., 2008) is presented in Figure 10. The input parameters and random variables used to generate the deterministic factor of safety as well as the probability of failure are summarized in a Table 3 for each model. As shown in Figure 10, the slope's failure surfaces are localized within the thick pile of overburden above the existing road level, indicating the influence of groundwater on the overall stability of the slopes which can worsen over time with the intensity of the rainfall in monsoon. The slope above the existing road level has two differentiated slopes. The

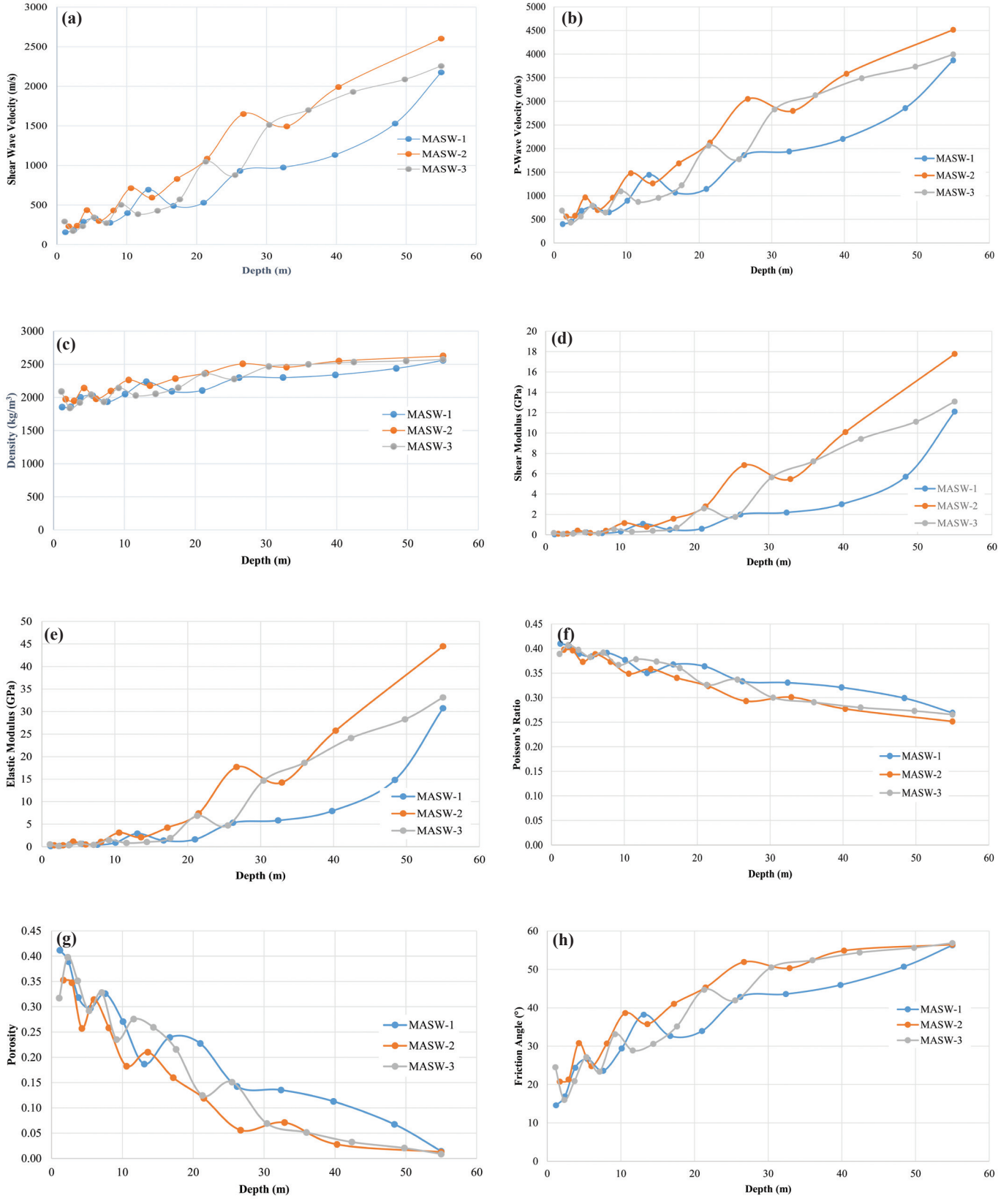

Fig 7: Graphical representation for dynamic properties of soil in terms of depth versus (a) shear wave velocity, (b) P-wave velocity, (c) density, (d) shear modulus, (e) elastic modulus, (f) poisson's ratio, (g) porosity, (h) friction angle.

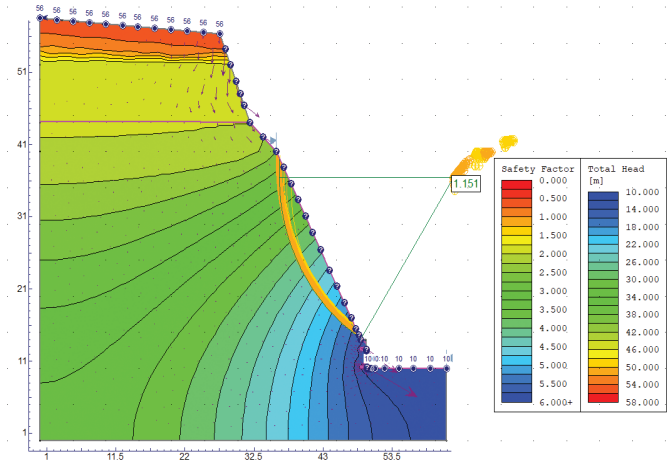

Fig. 8: Computed factor of safety for lower bench of model with marginal stability.

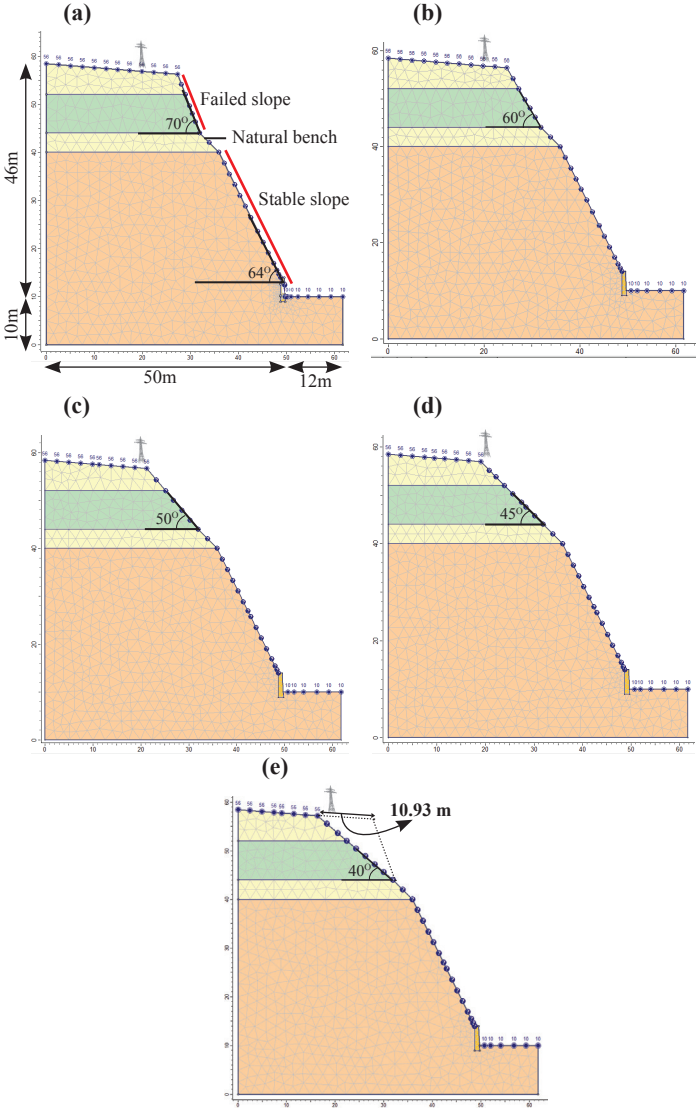

Fig. 9: Modification of failed slopes with respect to varying slope angles (a) 70° (present status), (b) 60°, (c) 50°, (d) 45°, (e) 40°. Vertical and horizontal scales are same for all figures.

upper slope is the failed slope and has attained a 70° slopes at the time of measurement. The lower stable slope has remained same as of the excavated slope of 64°. Because of this, the upper failed slope has been analyzed in detail so as to determine the factor of safety in different slope geometry and conditions. The slices of the queried slip surfaces (Fig. 10) showed potential shallow debris-slide in the study area rather than deep-seated landslides, which may be due to the steep gradient of the slope. This is consistent with the results and showed that a steep slope generally displays shallow failure, compared to a gentle slope with generally deep-seated landslides. The non-vegetation on the slope surface exposes the slope to surface erosion which may lead to local debris movement during the monsoon season.

In every instance of slope alteration, an assessment of slope stability has been conducted to ensure whether it reaches a secure state or not. The FoS has been computed for each type of limit equilibrium method (LEM), including Ordinary/ Fellenius, Bishop Simplified, Janbu Simplified, Janbu Corrected, Spencer, and Morgenstern-Price, as illustrated in Figure 10 and Table 3. Even after adjusting the slope angle from 70° to 40°, the factor of safety increased from 0.76 to 1.18 only. However, this increase in FoS is still insufficient to ensure the stability of the slope.

Modifying the slope angle from 70° to 40° resulted in the displacement of the slope edge inward by 10.9 meters. Consequently, the 132 kV transmission tower of Marsyangdi Corridor needs to be avoided. Therefore, it is recommended alternative stabilization techniques rather than further modifying the slope.

Various scenarios were examined by maintaining the failed slope as is and applying soil nails (Ø25 mm) of different lengths (3 m, 4.5 m, 6 m, 7.5 m, and 9 m) at 2 m spacing on its failed slope and a shear wall of 18-inch at its base. The input parameters for these soil nails were derived from laboratory testing and are given in Table 4. The results, as depicted in Figure 11 and summarized in Table 5, reveal that the factor of safety is satisfactory when using 6.0 m long soil nails, achieving a FoS of 1.3.

Table 3: Factor of safety in terms of variation of slope angles.

Slope	Limit equilibrium methods					
	OF	BS	JS	JC	S	MP
70°	0.777	0.762	0.783	0.807	0.774	0.775
60°	0.879	0.894	0.867	0.917	0.896	0.899
50°	0.983	1.013	0.968	1.025	1.010	1.011
45°	1.171	1.091	1.036	1.098	1.091	1.087
40°	1.171	1.176	1.116	1.183	1.173	1.171

OF = Ordinary/Fellenius, BS = Bishop Simplified, JS = Janbu Simplified, JC = Janbu Corrected, S = Spencer, and MP = Morgenstern-Price.

Table 4: Input parameters of soil nailing.

Type	FA	OPS (m)	TC (kN)	PC (kN)	PL (%)	BS (kN/m)
GT	AM	2	125.6	125.6	80	75.4

GT= grouted tieback, FA= force application, AM=active method, OPS= out-of-plane spacing, TC= tensile capacity, PC= plate capacity, PL= percent of length, BS= bond strength.

For 70° failed slope

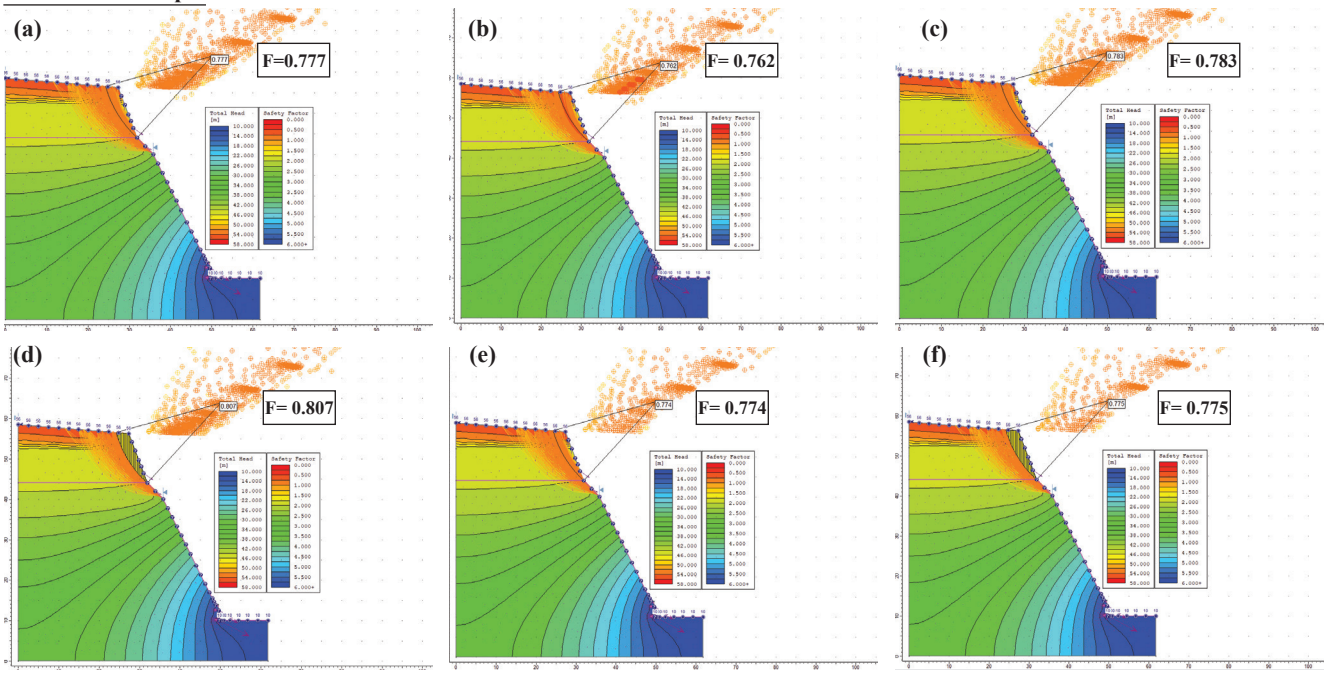

For 60° failed slope

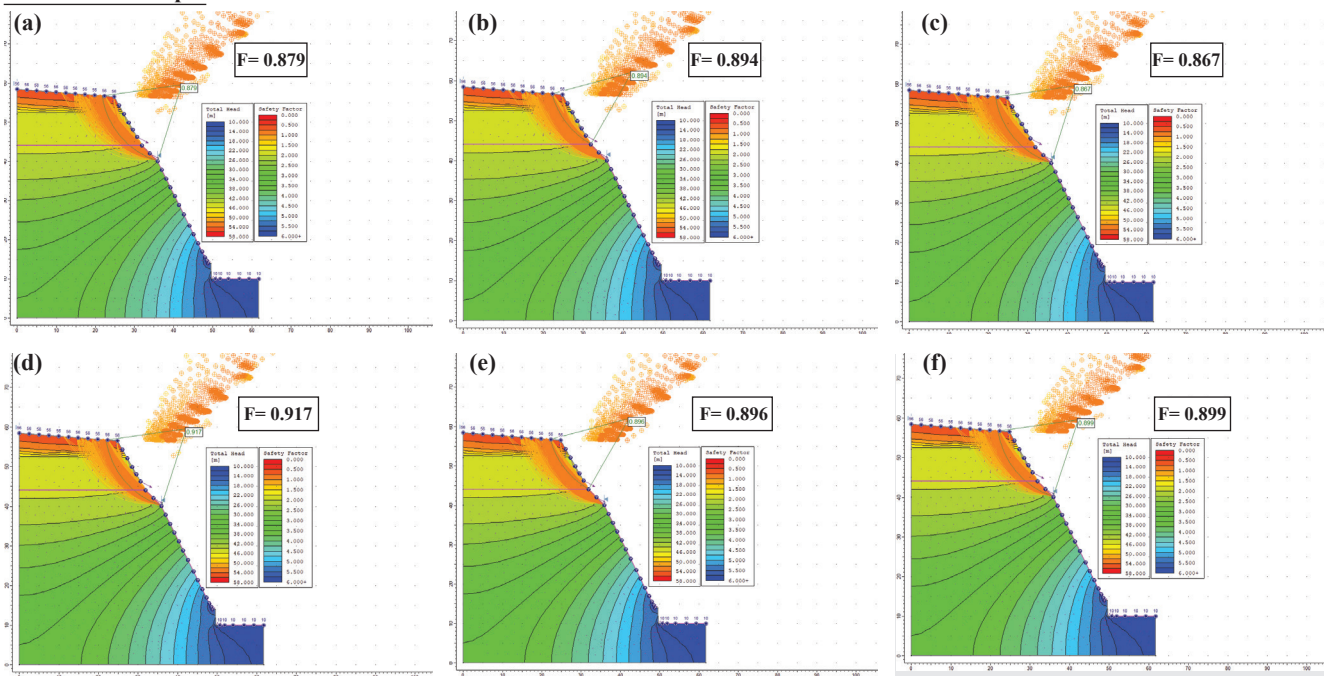

For 50° failed slope

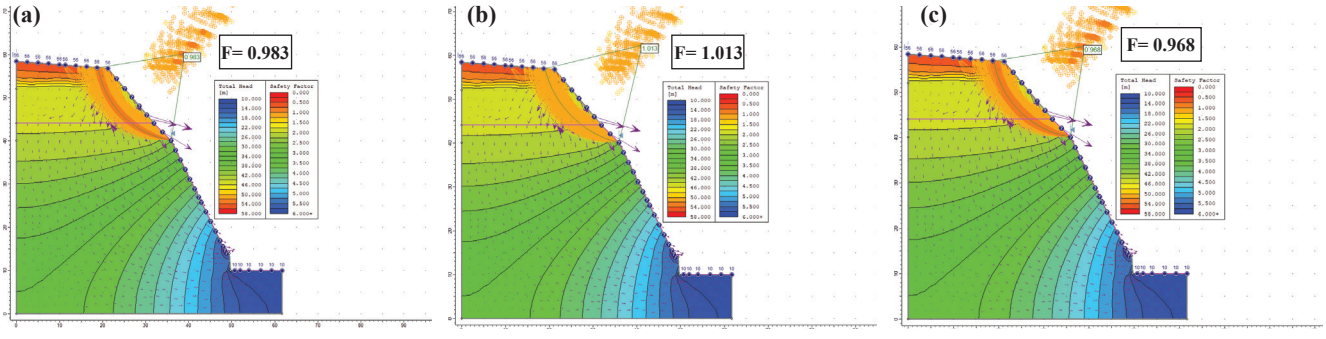

Fig. 10: Numerical modelling of cut-slopes by slope stability analysis methods (a) Ordinary/Fellenius, (b) Bishop Simplified, *(Contd...)*

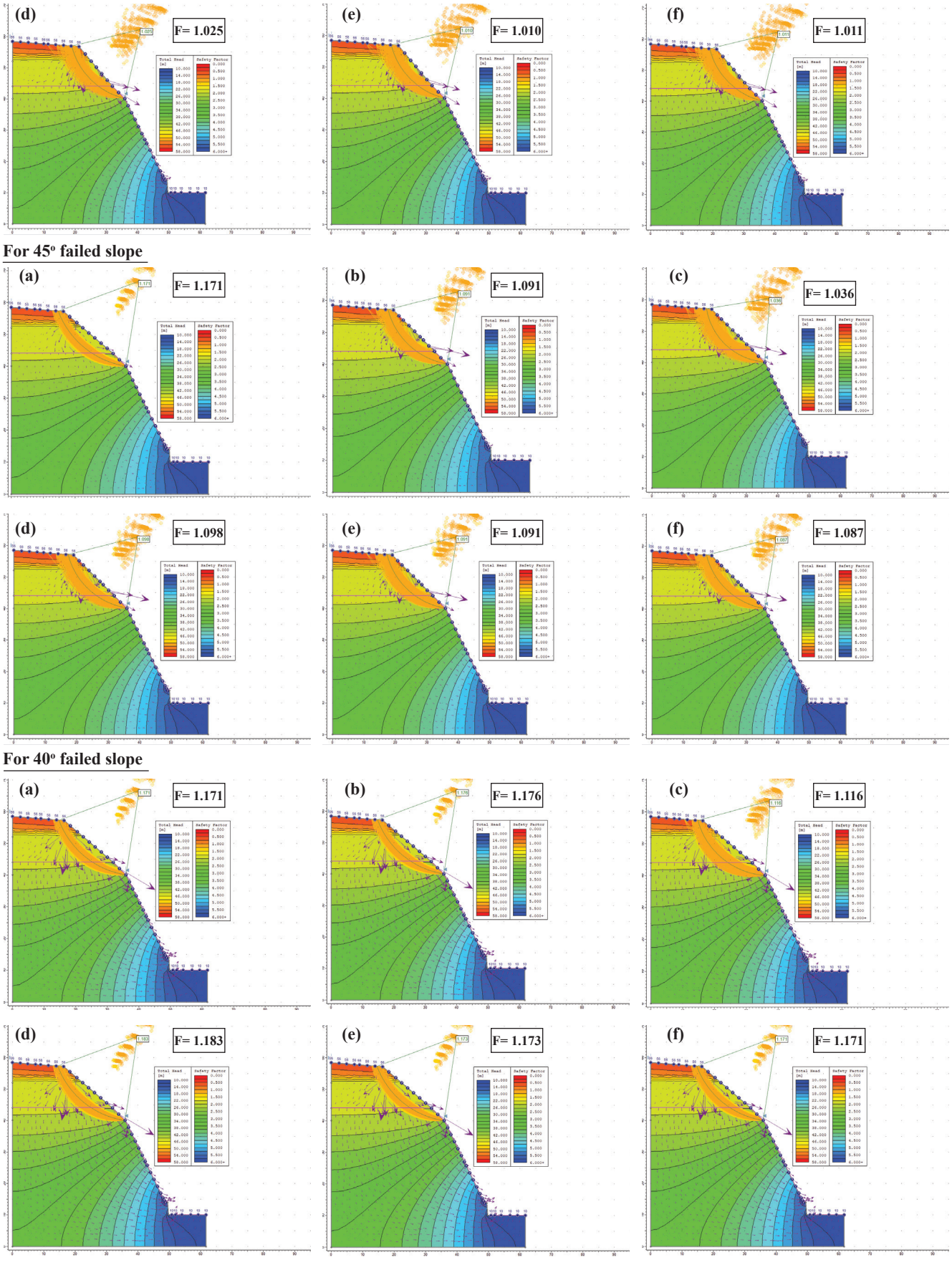

Fig. 10: Numerical modelling of cut-slopes by slope stability analysis methods (a) Ordinary/Fellenius, (b) Bishop Simplified, (c) Janbu Simplified, (d) Janbu Corrected, (e) Spencer, (f) GLE/Morgenstern-Price.

For 70° slope with 3.0 m soil nails

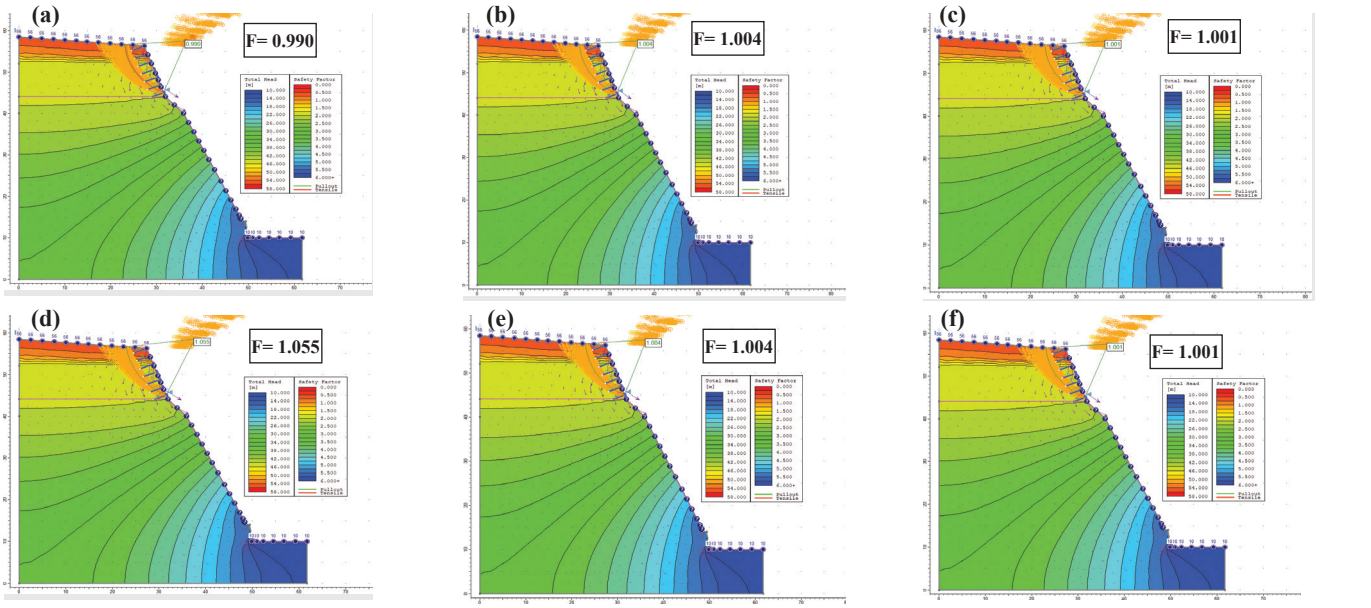

For 70° slope with 6 m soil nails

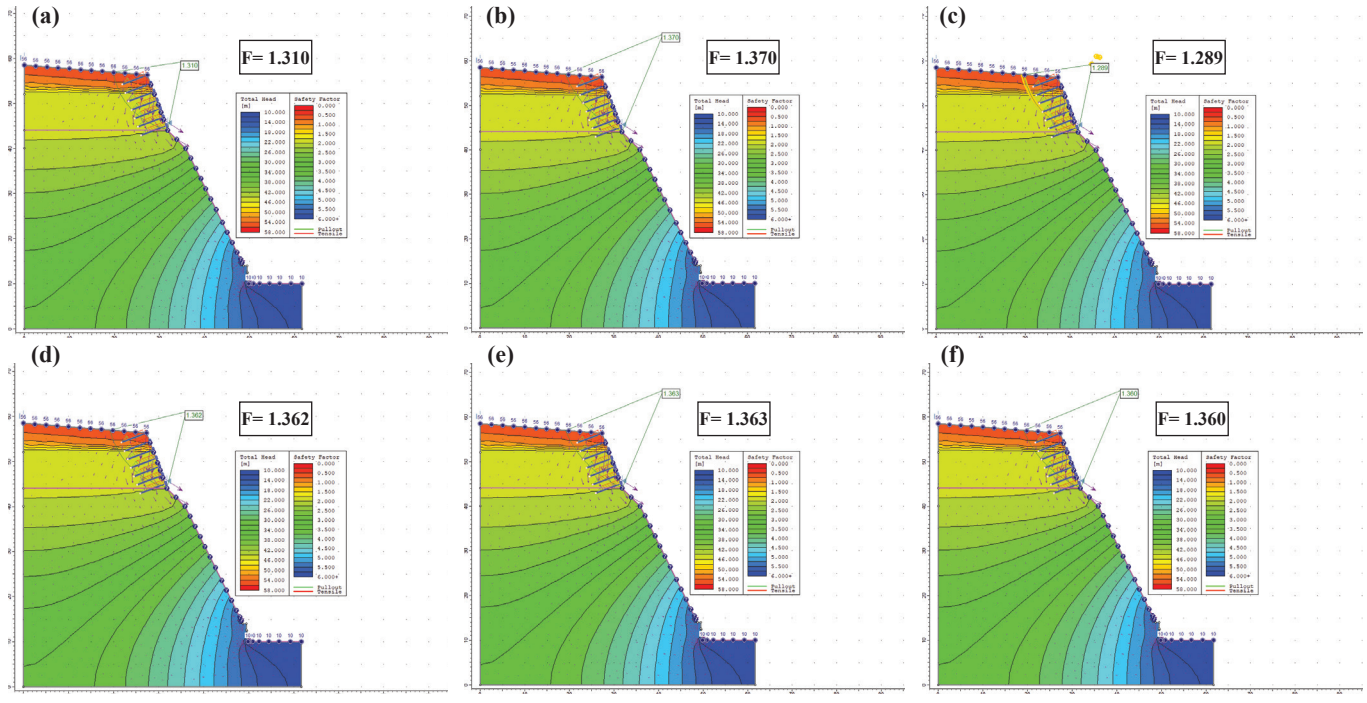

For 70° slope with 7.5 m soil nails

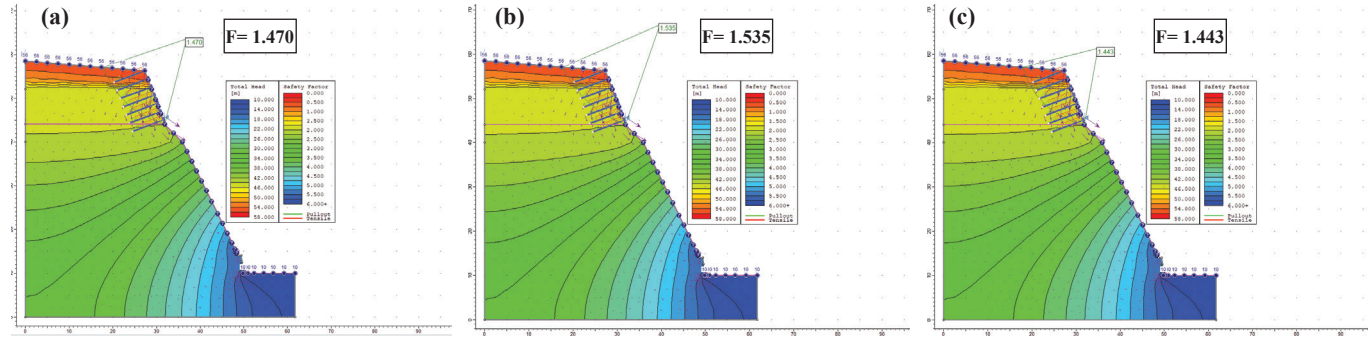

Fig. 11: Different lengths of soil nailing applied in slope stability analyses (a) Ordinary/Fellenius, (b) Bishop Simplified, (c) Janbu Simplified, (d) Janbu Corrected, (e) Spencer, (f) GLE/Morgenstern-Price. ***(Contd...)***

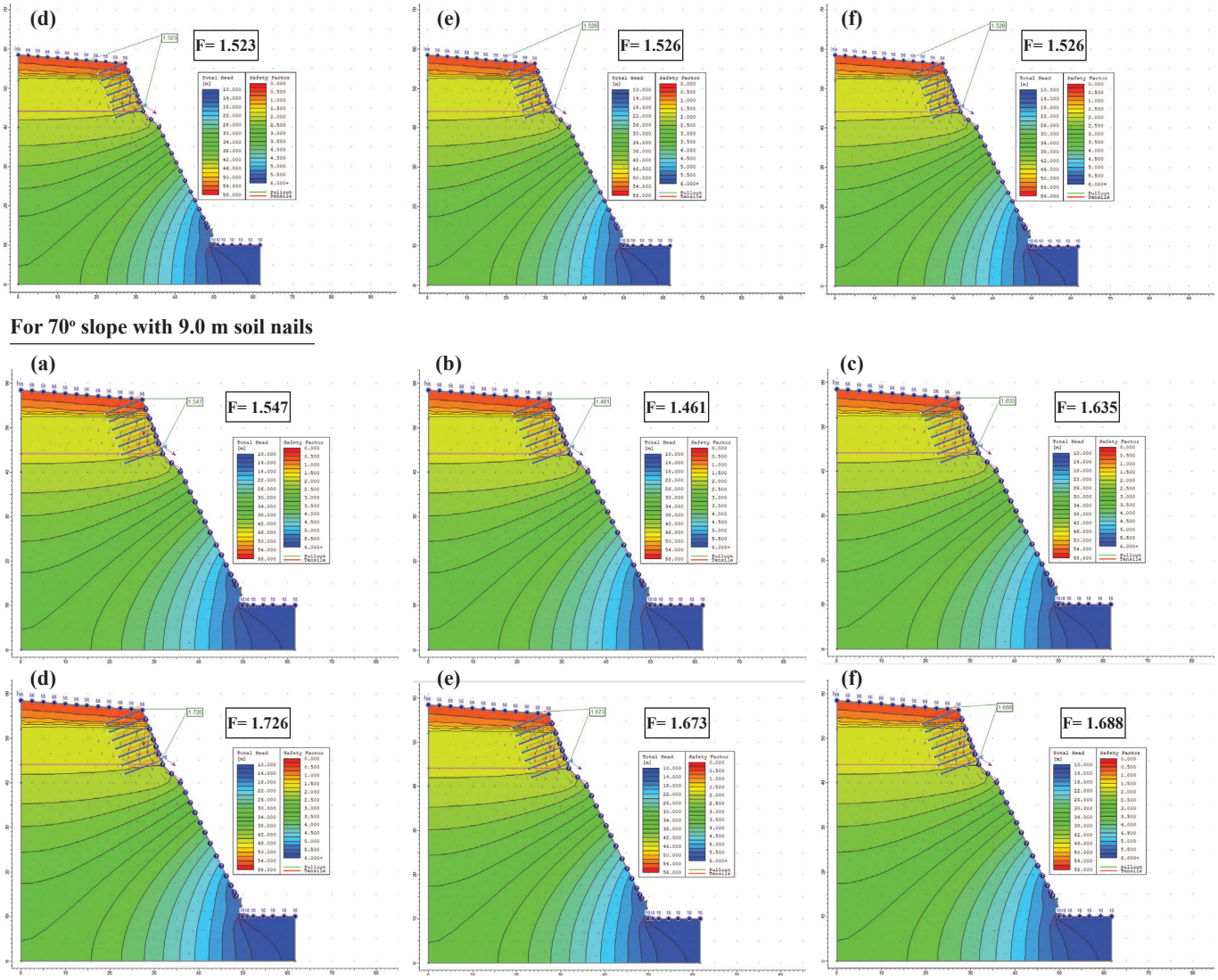

Fig. 11: Different lengths of soil nailing applied in slope stability analyses (a) Ordinary/Fellenius, (b) Bishop Simplified, (c) Janbu Simplified, (d) Janbu Corrected, (e) Spencer, (f) GLE/Morgenstern-Price.

Table 5: Factor of safety in terms of soil nailing lengths in existing failed slopes.

L	Limit equilibrium methods					
(m)	OF	BS	JS	JC	S	MP
3.0	0.990	1.004	1.001	1.055	1.004	1.001
4.5	1.152	1.206	1.138	1.196	1.196	1.192
6.0	**1.310**	**1.370**	**1.289**	**1.362**	**1.363**	**1.360**
7.5	1.470	1.535	1.443	1.523	1.526	1.526
9.0	1.547	1.461	1.635	1.726	1.673	1.688

L=length of soil nail, OF= Ordinary/Fellenius, BS= Bishop Simplified, JS= Janbu Simplified, JC= Janbu Corrected, S= Spencer, and MP= Morgenstern-Price.

The slope stability analysis were carried out using different methods of limit equilibrium methods considering both force and moment equilibrium conditions. The slope is considered safe once the FOS is above the minimum acceptable values of FOS. As per the EM 1110-2-1902, slope stability, other slopes, factor of safety and IS 456 2000, typical minimum acceptable values of factor of safety are about 1.3 for end of construction and multistage loading.

Finite Element Method (FEM)

The results of finite-element model based on existing slope (Fig.12a) and input parameters of soil nails as Table 4 are presented in Figure 12b,c,d,e and f. The interface between the sandy gravel and silty sand with gravel experiences the maximum shear strain at the base of the failed slope. Probably this contact zone represent the least resistant zone that ultimately favor the development of the sliding surface. It is therefore changing the slope geometry at this point could have a serious results on slope instability thereby creating slope failure continuously (Siddhique and Pradhan, 2018). Phase2 analysis method for the existing slope of the upper failed slope has analyzed the existing slope under the application of different lengths of soil nailing with properties as given in Table 4. Critical SRF for the existing failed slope under the application of 25 mm diameter soil nailing for 3.0 m, 4.5 m, 6.0 m, 7.5 m and 9.0 m lengths are 0.96, 1.15, 1.32, 1.43 and 1.62 respectively (Table 6). This indicates that the slope under the application of 3.0 m soil nailing is unstable yet whereas marginal stable under the application of 4.5 m long

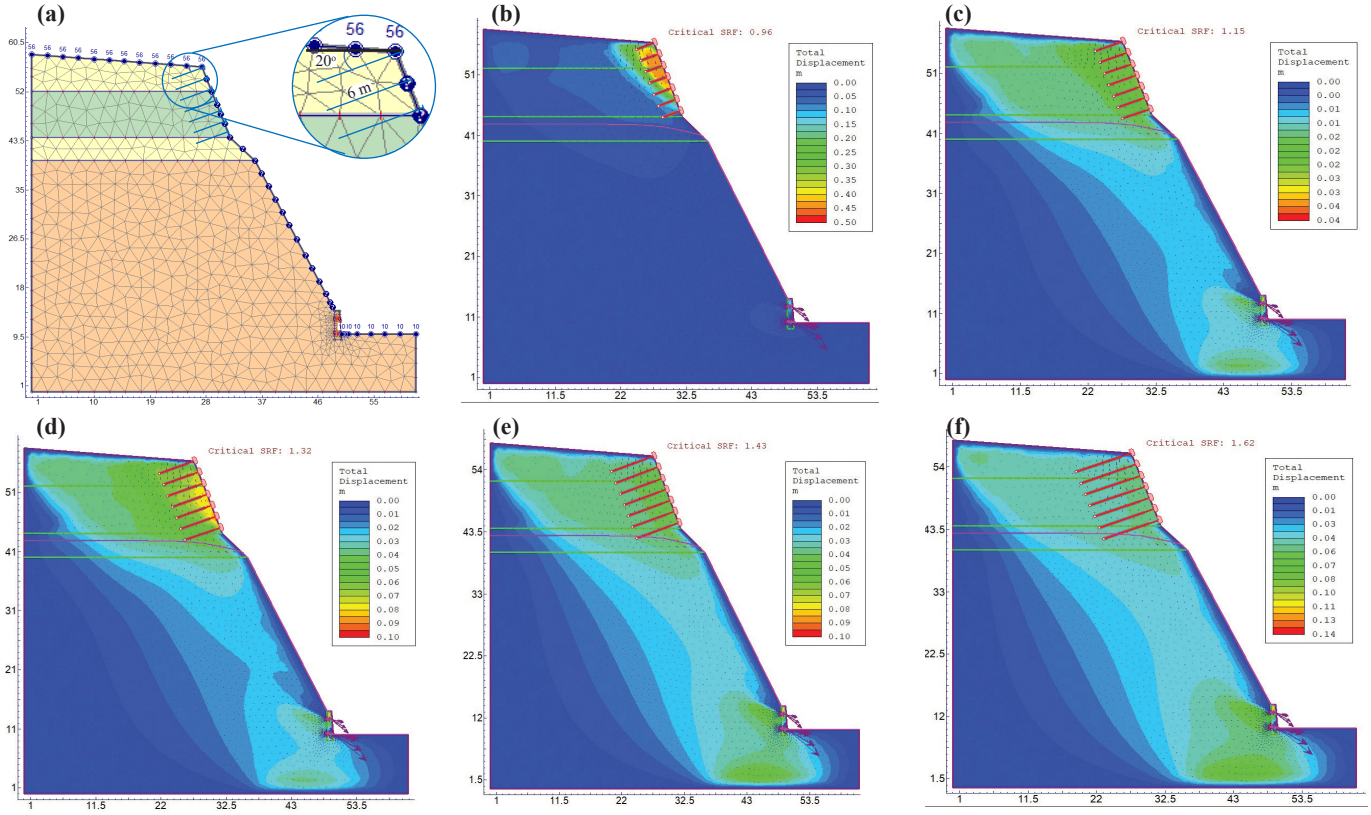

Fig. 12: Critical SRF of modelled cut-slopes in Phase2 (FEM) with the application of differential soil-nails (a) model set-up, (b) 3 m nails, (b) 4.5 m nails, (c) 6 m nails, (d) 7.5 m nails, (e) 9 m nails.

soil nailing. Since the critical SRF for the failed slope under the application of 6.0 m or longer soil nailing are greater than 1.3 and thus shows the slope stable.

Table 6: Strength reduction factor (SRF) for different lengths of soil nails.

Length of soil nailing, L (m)	Strength reduction factor (SRF)
3.0	0.96
4.5	1.15
6.0	1.32
7.5	1.43
9.0	1.62

Stability condition

The stability of a slope is influenced by a number of factors. In this study, it was found that the slopes' steep gradient for the upper silty sand and sandy gravel layer have weakened the slope stability. The compacted lower layer comprising of silty sand with gravels with low permeability hasn't affected the excavated cut-slope that much except sheet erosion at the exposed surface. This study provides evidence for a possible relation between the slope geometry (height of the failed slope) and its stability state. A low-height gentle slope for the failed slope experiences less gravitational loading and has better stability than a steep slope. With a FoS of 0.775 to 0.897 for slope angle of 70° and 60°, the cut-slope has demonstrated the unstable pre-failure condition. The modified slope for 50° and 40° has FoS more than unity in the range of 1.011 to 1.183 demonstrating marginally stable.

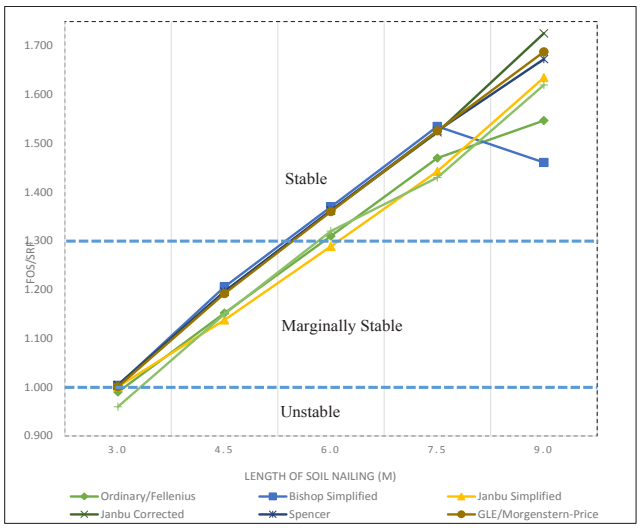

Fig. 13: Factor of Safety (FoS) and stress reduction factor (SRF) for different LEMs and FEM under the application of different soil nail lengths.

Importantly, altering the slope from 70° to 45° resulted in the inward shift of the upper slope's edge by 10.93 m, necessitating the specific relocation of a 120 kV transmission tower. The assessment of slope stability, conducted using limit equilibrium method and finite element method, revealed that soil nails, particularly those 6.0 meters or longer with grouted tiebacks, yielded a FoS exceeding 1.3 (Table 7), which is considered acceptable. Consequently, the implementation

Table 7: FoS/SRF values for varying lengths of soil nailing.

	Length (m) → Method↓	3.0	4.5	6.0	7.5	9.0
FoS/SRF	OF	0.990	1.152	**1.310**	1.470	1.547
	BS	1.004	1.206	**1.370**	1.535	1.461
	JS	1.001	1.138	**1.289**	1.443	1.635
	JC	1.005	1.196	**1.362**	1.523	1.726
	S	1.004	1.196	**1.363**	1.526	1.673
	MP	1.001	1.192	**1.360**	1.526	1.688
	FEM	0.960	1.150	**1.320**	1.430	1.620

OF = Ordinary/Fellenius, BS = Bishop Simplified, JS = Janbu Simplified, JC = Janbu Corrected, S = Spencer, and M P= Morgenstern-Price

of soil nailing for the upper failed slope emerges as a viable solution to enhance its stability and, by extension, the stability of the entire slope.

CONCLUSIONS

The failure of the modelled cut-slope in debris material is primarily governed by a combination of factors including slope geometry, height and shallow groundwater conditions. The absence of backfilling after the construction of the shear wall rendered it vulnerable to the forceful impact of the top failure of the cut slope, ultimately leading to its washout. A comprehensive slope stability analysis, employing various methods of limit equilibrium, has yielded valuable insights. Notably, modifying the failed slope, particularly the upper section, from an initial angle of 70° to 40° has significantly improved the factor of safety, elevating it from 0.762 to 1.183, rendering the slope marginally stable at 45°. However, this modification necessitates shifting the slope's edge inward by 10.93 meters and the relocation of 132 kV transmission towers, currently positioned at 8.0 meters from the existing slope edge. To preserve this critical infrastructure, soil nails with a diameter of 25 mm of various lengths, incorporating grouted tie backs were employed to analyze in both limit equilibrium method and finite element method that have consistently achieved an FoS of 1.3 or higher, which aligns with the minimum acceptable values stipulated by EM 1110-2-1902 and IS 456 2000 for end-of-construction and multistage loading scenarios. Therefore, the application of 25 mm diameter soil nails, each 6 m in length, spaced at 2 m intervals, featuring a tensile and plate capacity of 125.6 kN, a bond strength of 75.4 kN/m, and utilizing 80% of the length, has proven to be a successful solution in terms of slope stability. This approach ensures the safety and integrity of the slope, meeting or exceeding the established minimum safety criteria and safeguarding infrastructures located in its vicinity.

ACKNOWLEDGEMENT

We are thankful to Mr. D. B. Adhikary and Mr. M. R. Acharya for their technical assistance during this manuscript preparation.

REFERENCES

Albataineh, N., 2006, Slope stability analysis using 2D and 3D methods. M.Sc. thesis, Akron University, Ohio, USA.

Bieniawski, Z. T., 1989, *Engineering rock mass classification*. New York, John Wiley and Sons, Inc. 272 p.

Bishop, A. W., 1955, The use of failure circles in the stability analysis of slopes. Geotechnique, v. 5(1), pp. 7–17.

Brinkgreve, R. B. J, Engin, E., and Swolfs, W. M., 2013, Plaxis manual.

Chen, S., Yang, Z., Zhang, W., Li, L., Zheng, Y., and Yuan, Y., 2022, Numerical Simulation of the Stability of a Cutting Slope and Study on Its Reinforcement Scheme. Advances in Civil Engineering, v. 2022, 14 p.

Chen, S., Zhu, Y., Li, Z., Huang, L., and Zhang, H., 2014, Analysis of lateral slope stability during construction of a loess tunnel with a large section. Modern Tunnelling Technology, v. 51(1), pp. 82–89.

Cotecchia, F., 2003, Mechanical behaviour of the stiff clays from the Montemesola Basin in relation to their geological history and structure. Charact. Eng. Proper. Nat. Sediment., 2, pp. 817–850.

Dahal, R. K., 2012, Rainfall-induced landslides in Nepal. International Journal of Erosion Control Engineering, v. 5(1), pp. 1–5.

Dahal, R. K., Hasegawa, S., Masuda, T., and Yamanaka, M., 2006, Roadside slope failures in Nepal during torrential rainfall and their mitigation. Disaster mitigation of debris flows, slope failures and landslides, pp. 503–514.

Dahal, R., K., 2006, *Geology for Technical Students*. Bhrikuti Academic Publications, Kathmandu, Nepal, 746 p.

Duncan, J. M., 1996, State of the art: limit equilibrium and finite-element analysis of slopes. Journal of Geotechnical and Geoenvironmental Engineering, 122(7), pp. 557–596.

Elahi, T. E., Islam, M. A., and Islam M. S., 2022, Parametric Assessment of Soil Nailing on the Stability of Slopes Using Numerical Approach. Geotechnics, v. 2, pp. 615–634.

EM 1110-2-1902, 2023, Engineers Manual on Slope Stability. US Army Corps of Engineers, Engineering and Design.

Fan, C. C. and Luo, J. H., 2008, Numerical study on the optimum layout of soil–nailed slopes. Computational Geotechnics, v. 35, pp. 585–599.

Fan, Q., Lin, J., Sun, W., Lu, J., and Chen, P., 2021, Analysis of landslide stability based on the Morgenstern–Price method. E3S Web of Conferences, 299, 02019.

Fawaz, A., Farah, E., and Hagechechade, F., 2014, Slope stability analysis using numerical modelling. American Journal of Civil Engineering, v. 2(3), pp. 60–67.

Fellenius, W., 1936, Calculation of the stability of earth dams. In Trans., 2nd Congress on Large Dams. U.S. Government Printing Office, Washington, DC, pp. 445–462.

Griffiths, D. V. and Lane, P. A., 1999, Slope stability analysis by finite elements. Geotechnique, v. 49(3), pp. 387–403.

IS Standard 2720–13, 1986, Methods of test for soils, part 13: Direct shear test (CED 43: Soil and G\Foundation Engineering).

IS Standard 456 2000, 2007, Plain and Reinforced Concrete- Code of Practice (CED 2: Cement and Concrete.

Jaiswal, S., Srivastava, A., and Chauhan, V. B., 2022, Numerical Modeling of Soil-Nailed Slope Using Drucker–Prager Model. In: Choudhary, A. K., Mondal, S., Metya, S., and Babu, G. L. S. (eds.), Advances in Geo-Science and Geo-Structures, Lecture Notes in Civil Engineering, v. 154, Springer.

Janbu, N., 1954, Application of composite failure surface for stability analysis. Proc., European Conf. on Stability of Earth Slopes, International Society of Soil Mechanics and Geotechnical Engineering (ISSMGE), London, pp. 1–16.

Kainthola, A., Singh, P. K., Wasnik, A. B., Sazid, M., and Singh, T. N.,

2012, Distinct element modelling of Mahabaleshwar road cut hill slope. Int. Jour. Geomaterials, 2, pp. 105–113.

Kassab, M. A. and Weller, A., 2014, Study on P-wave and S-wave velocity in dry and wet sandstone of Tushka region, Egypt. Egyptian Journal of Petroleum, v. 28(1), pp. 1–11.

Kharel, G. and Acharya, I. P., 2017, Stability Analysis of Cut-slope: A case study of Kathmandu–Nijghad Fast track. Proceedings of IOE Graduate Conference, v. 5, pp. 171–174.

Lenti, L., Semblat, J. F., Delepine, N., and Bonnet, G., 2008, Dynamic Soil Response for Strong Earthquakes: A Simplified Nonlinear Constitutive Model. In The 14th World Conference on Earthquake Engineering, Beijing, China.

Li, Z. and Wang, J., 2007, Lower bound limit study on plastic limit analysis of rock slope using finite elements based on nonlinear programming. Chinese Journal of Rock Mechanics and Engineering, v. 4, pp. 747–753.

Lin, H., Xiong, W., and Cao, P., 2013, Stability of soil nailed slope using strength reduction method. European Journal of Environmental and Civil Engineering, v. 17, pp. 872–885.

Loke, M. H. and Lane, J. W., 2004, Inversion of data from electrical resistivity imaging surveys in water-covered areas. Exploration Geophysics, 35, pp. 266–271.

Loroueil, S. and Hight, D. W., 2003, Behaviour and properties of natural sediments and soft rocks. Charact. Eng. Proper. Nat. Sediment., 2, pp. 29–254.

Matsui, T. and San, K. C., 1992, Finite element slope stability analysis by shear strength reduction technique. Soils Found., v. 32(1), pp. 59–70.

May, D. R. and Brahtz, H. A., 1936, Proposed Methods of Calculating the Stability of Earth Dams. Trans. 2nd Cong. on Large Dams, v. 4, 539 p.

Miščević, P. and Vlastelica, G., 2014, Impact of weathering on slope stability in soft rock mass. Journal of Rock Mechanics and Geotechnical Engineering, v. 6(3), pp. 240–250.

Morgenstern, N. U. and Price, V. E., 1965, The analysis of the stability of general failure surfaces. Geotechnique, v. 15(1), pp. 79–93.

Nie, Z., Zhang, Z., and Zheng, H., 2019, Slope stability analysis using convergent strength reduction method. Engineering Analysis with Boundary Elements, v. 108, pp. 402–410.

Pandey, A., Jaiswal, S., and Chauhan, V. B., 2021, Numerical Studies on the Behavior of Slope Reinforced with Soil Nails. In: Sitharam, T. G., Jakka, R., and Govindaraju, L. (eds.), Local Site Effects and Ground Failures, Lecture Notes in Civil Engineering, v. 117, Springer.

Park, C. B., Miller, R. D., and Xia, J., 1999, Multichannel analysis of surface waves. Geophysics, v. 64(3), pp. 800–808.

Pradhan, S. P. and Siddique, T., 2018, Stability and sensitivity analysis of Himalayan road cut debris slopes: an investigation along NH-58, India. Natural Hazards, v. 93(2), pp. 577–600.

Pradhan, S. P., Siddique, T., and Ansari, T. A., 2020, Stability assessment of landslide-prone road cut rock slopes in Himalayan terrain: a finite element method based approach. Journal of Rock Mechanics and Geotechnical Engineering, 12, pp. 59–73.

Pradhan, S. P., Vishal, V., Singh, T. N., and Singh, V. K., 2014, Optimization of Dump Slope Geometry vis-a-vis Flyash Utilization Using Numerical Simulation. American Journal of Mining and Metallurgy, v. 2(1), pp. 1–7.

Rawat, S., Zodinpuii, R., Manna, B., and Sharma, G., 2013, Investigation on the failure mechanism of nailed slopes under surcharge loading: Testing and analysis. Geomechanics and Geoengineering, v. 9, pp. 18–35.

Rocscience Inc., 2001-2004, SLIDE Version 6. Probabilistic Analysis Tutorial. Toronto: Rocscience Inc.

Shah, S. S. A., Asif, A. R., Ahmed, W., Islam, I., Waseem, M., Janjuhah, H. T., and Kontakiotis, G., 2023, Determination of Dynamic Properties of Fine-Grained Soils at High Cyclic Strains. Geosciences, v. 13, 204 p.

Shah, S. S. A., Asif, A. R., Ahmed, W., Islam, I., Waseem, M., Janjuhah, H. T., and Kontakiotis, G., 2023, Determination of Dynamic Properties of Fine-Grained Soils at High Cyclic Strains. Geosciences, v. 13, 204 p.

Sharma, L. K., Umrao, R. K., Singh, R., Ahmad, M., and Singh, T. N., 2016, Geotechnical Characterization of Road Cut Hill Slope Forming Unconsolidated Geo-materials: A Case Study Geotech. Geol. Eng.

Siddique, T. and Pradhan, S. P., 2018, Stability and sensitivity analysis of Himalayan road cut debris slopes: An investigation along NH-58, India. Natural Hazards, v. 93(2), pp. 577–600.

Siddique, T., 2018, Slope Stability Investigations of Road Cut-slopes along NH-58, Rishikesh to Devprayag. Indian Institute of Technology Roorkee (IITR).

Siddique, T., Masroor Alam, M., Mondal, M. E. A., and Vishal, V., 2015, Slope mass rating and kinematic analysis of slopes along the national highway-58 near Jonk, Rishikesh, India. Journal of Rock Mechanics and Geotechnical Engineering, v. 7(5), pp. 600–606.

Siddique, T., Pradhan, S. P., Vishal, V., and Singh, T. N., 2017, Stability assessment of Himalayan road cut slopes along National Highway-58, India. Environ. Earth Sci., 76, p. 759.

Singh T. N., Gulati, A., Dontha, L., and Bhardwaj, V., 2008, Evaluating cut slope failure by numerical analysis-a case study. Nat. Hazards, 47, pp. 263–279.

Singh, H. O., Ansari, T. A., Singh, T. N., and Singh, K. H., 2020, Analytical and numerical stability analysis of road cut-slopes in Garhwal Himalaya, India. Geotechnical and Geological Engineering, v. 38(5), pp. 4811–4829.

Singh, T. N., Pradhan, S. P., and Vishal, V., 2013, Stability of slopes in a fire-prone mine in Jharia Coalfield, India. Arab. Jour. Geosci., v. 6(2), pp. 419–427.

Spencer, E., 1967, A Method of Analysis of the Stability of Embankments Assuming Parallel Inter-Slice Forces. Geotechnique, v. 17(1), pp. 11–26.

Stark, T. D., Choi, H., and McCone, S., 2005, Drained shear strength parameters for analysis of landslides. Jour. Geotech. Geoenviron. Eng., v. 131(5), pp. 575–588.

Strelec, S., Stanko, D., and Gazdek, M., 2016, Empirical Correlation between the Shear-Wave Velocity and the Dynamic Probing Heavy Test: Case Study, Varaždin, Croatia. Acta Geotechnica Slovenica, v. 13(1), pp. 3–15.

Sutejo, Y. and Gofar, N., 2015, Effect of Area Development on the Stability of Cut Slopes. The 5th International Conference of Euro Asia Civil Engineering Forum (EACEF-5), Procedia Engineering, 125, pp. 331–337.

Swan, C. C., and Seo, Y. K., 1999, Limit state analysis of earthen slopes using dual continuum/FEM approaches. Int. Jour. Numer. Anal. Methods Geomech., v. 23(12), pp. 359–1371.

Towhata, I., 1996, Seismic Wave Propagation in Elastic Soil with Continuous Variation of Shear Modulus in the Vertical Direction. Soils and Foundations, v. 36(1), pp. 61–72.

Umrao, R. K., Singh, R., Ahmad, M., and Singh, T. N., 2011, Stability analysis of cut slopes using continuous slope mass rating and kinematic analysis in Rudraprayag district, Uttarakhand. Geomaterials, 1, pp. 79–87.

Valentino, R., Sobio, Y., Mizero, J., Safari, J., and Nsengiyumva, F., 2021, Unstable road cut slopes and design of retaining structures in the Rwandan context. Arabian Journal of Geosciences, 14, 1405 p.

Wang, H., Zhang, B., Mei, G., and Xu, N., 2019, A statistics-based discrete element modeling method coupled with the strength reduction method for the stability analysis of jointed rock slopes.

Engineering Geology, v. 264, Article ID 105247.

Wei, Y., Jiaxin, L., Zonghong, L., Wei, W., and Xiaoyun, S., 2020, A strength reduction method based on the Generalized Hoek- Brown (GHB) criterion for rock slope stability analysis. Computers and Geotechnics, v. 117, Article ID 103240.

Weingarten, J. S. and Perkins, T. K., 1995, Prediction of sand production in gas wells: methods and Gulf of Mexico case studies. Journal of Petroleum Technology, pp. 596–600.

Wyllie, D. C. and Mah, C. W., 2004, Rock slope engineering. In: Hoek, E. and Bray, J. W. (eds.) Rock slope engineering, 4th Ed., Taylor and Francis Group, London.

Yang, Y., Sun, G., Zheng, H., and Qi, Y., 2019, Investigation of the sequential excavation of a soil-rock-mixture slope using the numerical manifold method. Engineering Geology, v. 256, pp. 93–109.

Zainorabidin, A. and Mad Said, M. J., 2015, Determination of Shear Wave Velocity Using Multi-channel Analysis of Surface Wave Method and Shear Modulus Estimation of Peat Soil at Western Johore. Procedia Engineering, v. 125, pp. 345–350.

Zhang, G., Cao, J., and Wang, L., 2014, Failure behavior and mechanism of slopes reinforced using soil nail wall under various loading conditions. Soils and Foundations, v. 54, pp. 1175–1187.